The nucleophilic displacement reactions[15] summarized by eq 5 proceed through short-lived orange intermediates, which we have not as yet been able to characterize spectroscopically. However, by analogy to the substitution processes outlined in eq 1, we believe that the first step in reactions 5 is probably the formation of an η^1-C_5H_5 complex, the orange intermediate, i.e.

$$[(\eta^5\text{-}C_5H_5)M(NO)I(PMe_3)_2]I + 2PMe_3 \rightarrow [(\eta^1\text{-}C_5H_5)M(NO)(PMe_3)_4]^+I^- \quad (6)$$

The seven-coordinate cationic complex thus formed could then undergo nucleophilic attack by PMe_3 at the η^1-cyclopentadienyl ring to afford the final products, i.e.

$$[(\eta^1\text{-}C_5H_5)M(NO)(PMe_3)_4]^+I^- + PMe_3 \rightarrow M(NO)(PMe_3)_4I + [(C_5H_5)PMe_3]I \quad (7)$$

It is interesting to compare reactions 7, in which the C_5H_5 group is formally displaced as a cation, with the transformation involving a valence isoelectronic rhenium reactant, i.e.[4]

$$(\eta^1\text{-}C_5H_5)Re(NO)(PMe_3)_3Me + PMe_3 \rightarrow [Re(NO)(PMe_3)_4Me]^+C_5H_5^- \quad (8)$$

in which the C_5H_5 ligand is liberated from the coordination sphere of the metal as an anion. It thus appears that for these systems, the mode of reactivity of PMe_3 with the cyclopentadienyl-containing reactant is governed by the requirement that the final tetrakis(phosphine) product complexes each satisfy the familiar 18-valence-electron rule.

From a practical point of view, the most convenient method for the synthesis of the $M(NO)(PMe_3)_4I$ complexes is the direct treatment of the $[(\eta^5\text{-}C_5H_5)M(NO)I_2]_2$ (M = Mo, W) dimers with 10 equiv of PMe_3, i.e.

$$[(\eta^5\text{-}C_5H_5)M(NO)I_2]_2 + 10PMe_3 \xrightarrow{CH_3CN} 2M(NO)(PMe_3)_4I + 2[(C_5H_5)PMe_3]I \quad (9)$$

Obviously, reactions 9 are simply the sums of the conversions shown in eq 3–5, and they do afford the desired $M(NO)(PMe_3)_4I$ (M = Mo, W) products in good yields. The characteristic chemistry of these electron-rich nitrosyl complexes is currently being investigated.

In closing, one final point concerning the reactions of the $[(\eta^5\text{-}C_5H_5)M(NO)I_2]_2$ dimers with PMe_3 must be made. In the presence of an added reducing agent such as sodium amalgam, the two reactants do not produce the $M(NO)(PMe_3)_4I$ complexes considered above. Instead, the reaction that occurs under these experimental conditions is as shown in eq 10, i.e.

$$[(\eta^5\text{-}C_5H_5)M(NO)I_2]_2 + 4Na/Hg + 4PMe_3 \xrightarrow{THF} 2(\eta^5\text{-}C_5H_5)M(NO)(PMe_3)_2 + 4NaI + Hg \quad (10)$$

the final $(\eta^5\text{-}C_5H_5)M(NO)(PMe_3)_2$ (M = Mo, W) complexes being isolable in excellent yields as orange, crystalline solids. Conversions 10 are particular examples of a general mode of reactivity that we have described in some detail previously.[9] The new $(\eta^5\text{-}C_5H_5)M(NO)(PMe_3)_2$ compounds are formally related to the $M(NO)(PMe_3)_4I$ complexes and, like them, are very air- and moisture-sensitive and decompose in chlorinated organic solvents. The spectroscopic properties of these compounds (Table I) are consistent with their possessing the familiar "three-legged piano-stool" molecular structures.[9] Of particular interest are the very low nitrosyl-stretching frequencies evident in their IR spectra [e.g. ν_{NO} (CH_2Cl_2) 1523 and 1510 cm^{-1} for M = Mo and W, respectively], a feature that again emphasizes the electron richness of the group 6 metal centers in these complexes.

Acknowledgment. We are grateful to the Natural Sciences and Engineering Research Council of Canada for support of this work in the form of grants to P.L. and a graduate scholarship to A.D.H. In addition, L.S. acknowledges the Spanish Ministry of Education for the award of a postdoctoral fellowship.

Registry No. $(\eta^5\text{-}C_5H_5)Mo(NO)I_2(PMe_3)$, 110015-39-9; $(\eta^5\text{-}C_5H_5)W(NO)I_2(PMe_3)$, 110044-52-5; $[(\eta^5\text{-}C_5H_5)Mo(NO)I(PMe_3)_2]I$, 110015-40-2; $[(\eta^5\text{-}C_5H_5)W(NO)I(PMe_3)_2]I$, 110015-41-3; $Mo(NO)(PMe_3)_4I$, 110015-42-4; $W(NO)(PMe_3)_4I$, 110015-43-5; $(\eta^5\text{-}C_5H_5)Mo(NO)(PMe_3)_2$, 110015-44-6; $(\eta^5\text{-}C_5H_5)W(NO)(PMe_3)_2$, 110015-45-7; $[(\eta^5\text{-}C_5H_5)Mo(NO)I_2]_2$, 12203-25-7; $[(\eta^5\text{-}C_5H_5)W(NO)I_2]_2$, 71341-43-0; $[(C_5H_5)PMe_3]I$, 110015-46-8; PMe_3, 594-09-2.

---

[15] Related displacements of a cyclopentadienyl ligand by other nucleophiles have been reported; for representative examples, see: (a) Mawby, R. J.; White, C. *J. Chem. Soc., Chem. Commun.* **1968**, 312. (b) White, C.; Mawby, R. J. *Inorg. Chim. Acta* **1970**, *4*, 261. (c) Kita, W. G.; McCleverty, J. A.; Patel, B.; Williams, J. *J. Organomet. Chem.* **1974**, *74*, C9. (d) McCleverty, J. A.; Williams, J. *Transition Met. Chem.* (*Weinheim, Ger.*) **1976**, *1*, 288. (e) Avilés, T.; Royo, P. *J. Organomet. Chem.* **1981**, *221*, 333. (f) Slocum D. W.; Engelmann, T. R.; Fellows, R. L.; Moronski, M.; Duraj, S. *J. Organomet. Chem.* **1984**, *260*, C21 and references cited therein.

Contribution from the Institute of Industrial Science,
University of Tokyo, 22-1 Roppongi, 7 Chome, Minato-ku, Tokyo 106, Japan

Cis Influence on Nuclear Spin–Spin Coupling Constants and Metal–Ligand Bonding Properties in Tin(II)-Coordinated Transition-Metal Complexes

Tetsu Yamakawa, Hiroshi Moriyama, Sumio Shinoda, and Yasukazu Saito*

Received November 3, 1986

Geminal ^{119}Sn–^{117}Sn nuclear spin–spin coupling constants of transition-metal complexes with chemically equivalent but magnetically nonequivalent trichlorostannate ($SnCl_3^-$) ligands have been satisfactorily correlated with orbital characteristics of the specific occupied and unoccupied molecular orbitals in the Pople–Santry framework by the extended Hückel method. The orbital energy of the axial ligand was important for determining the magnitude of the geminal coupling constants between the trans-disposed tin(II) ligands on the equatorial plane of the octahedral complexes. The ^{99}Ru–^{119}Sn one-bond coupling constants and the bonding properties of the metal–ligand coordination were also discussed from the viewpoint of the cis influence.

Introduction

Nuclear spin–spin coupling constants in coordination compounds provide valuable information not only on the molecular structures,[1,2] static and dynamic, but also on the metal–ligand bonding properties.[3] This molecular information has attracted special

---

* To whom correspondence should be addressed.

[1] Davis, J. A. In *The Chemistry of the Metal–Carbon Bond*; Hartley, F. R., Patai, S., Eds.; Wiley: New York, 1982; Vol. 1, p 813 and references therein.

0020-1669/87/1326-3347$01.50/0

Table I. Valence s Electron Density of Coordinated Tin(II) Atoms in Tin(II)-Coordinated Transition-Metal Complexes Calculated by EHMO within a Pople–Santry Framework

complex	$[s(0)]^2$/au eq	$[s(0)]^2$/au ax
$[Ru(SnCl_3)_6]^{4-}$	32.9	
$[RuCl(SnCl_3)_5]^{4-}$	36.2	26.1
trans-$[RuCl_2(SnCl_3)_4]^{4-}$	36.6	...
$[Os(SnCl_3)_6]^{4-}$	32.7	
$[OsCl(SnCl_3)_5]^{4-}$	36.0	19.9
$[RhH(SnCl_3)_5]^{3-}$	38.9	31.1
trans-$[IrCl_2(SnCl_3)_4]^{3-}$	39.1	...
cis-$[IrCl_2(SnCl_3)_4]^{3-}$	36.9	34.2
$[IrH(SnCl_3)_5]^{3-}$	36.0	24.9
trans-$[IrClH(SnCl_3)_4]^{3-}$	38.0	...
cis-$[PdCl_2(SnCl_3)_2]^{2-}$	11.5	
$[Pt(SnCl_3)_4]^{2-}$	68.2	
$[PtCl(SnCl_3)_3]^{2-}$	65.6[b]	14.9[c]
cis-$[PtCl_2(SnCl_3)_2]^{2-}$	17.8	
SCF value[a]	15.3	

[a] See text. [b] Trans to Sn. [c] Trans to Cl.

interest from the theoretical viewpoint for the following reasons: (i) many of compounds with NMR active nuclei become the objects of observation, (ii) NMR spin coupling constants are sensitive to coordination structures and to the influence of the metal species and ligands, and (iii) the mechanism of spin coupling is dominated usually by the Fermi contact term in coordination compounds.[4] Various quantum chemical approaches were attempted, therefore, to understand the bonding properties of the metal–ligand coordination.

With regard to the metal–ligand spin coupling constants, extensive knowledge has been accumulated for the trans influence,[5] while the cis influence, small in magnitude and rather irregular, was only observed for some square-planar platinum(II)[5,6] and octahedral tungsten(0) complexes.[7]

Table II. Geminal Tin–Tin and Phosphorus–Phosphorus Coupling Constants (^2J), Reduced Ones (^2K), and Corresponding Mutual Polarizabilities ($^2\pi$) of Platinum(II) Complexes

complex	$^2J^a$/Hz trans	$^2J^a$/Hz cis	$^2K^a/10^{21}$ cm^{-3} trans	$^2K^a/10^{21}$ cm^{-3} cis	$^2\pi/10^{-3}$ eV^{-1} trans	$^2\pi/10^{-3}$ eV^{-1} cis
$[Pt(SnCl_3)_4]^{2-}$	29 882	1835	1870	115	+2.55	−0.13
$[PtCl(SnCl_3)_3]^{2-}$	43 689	2039	2740	128	+3.71	−0.76
cis-$[PtCl_2(SnCl_3)_2]^{2-}$		2564		161		−1.55
$[PtCl(PMe_3)_3]^+$	+414	−25	+21.0	−1.27	+0.75	−0.35

[a] Signs undetermined for the nuclear spin coupling constants and the reduced ones of tin(II)-coordinated complexes.

In the present work, the one-bond metal–tin and geminal tin–tin coupling constants are investigated to elucidate the coordination properties in some tin(II)-coordinated square-planar and octahedral transition-metal complexes from the viewpoint of ligand mutual influence.

Calculations

One-electron wave functions and energies were calculated according to the extended Hückel molecular orbital method, with a charge iterative procedure at the sensitivity of 2 eV/charge for all atoms included. Slater-type functions were used as the valence atomic orbitals and their ionization potentials allotted to the diagonal terms (Coulomb integrals). The off-diagonal elements (resonance integrals) were evaluated by the Wolfsberg–Helmholtz expression ($K = 1.75$).[8]

The bond distances and angles in the complexes were taken from the X-ray analysis[2b,2f,9] of $[RuCl(SnCl_3)_5]^{4-}$, $[OsCl(SnCl_3)_5]^{4-}$, and *cis*-$[PtCl_2(SnCl_3)_2]^{2-}$ in the corresponding parts. The Rh–H and Ir–H distances in the hydride complexes were set as 1.48 Å, taken from the Rh–H value of $[RhClH(SiCl_3)(PPh_3)_2]$.[10]

The molecular orbitals responsible for the nuclear spin–spin coupling constants were simplified plainly by substituting the s and p orbitals of chlorine in the $SnCl_3^-$ ligand with the s orbital of hydrogen in the symbolic SnH_3^- expression, where the Slater exponent of hydrogen was taken as 1.40 so that the charge of the tin atom in SnH_3^- was the same as that in $SnCl_3^-$. It was confirmed beforehand for the typical set of *trans*-$[RuCl_2(SnCl_3)_4]^{4-}$ and *trans*-$[RuCl_2(SnH_3)_4]^{4-}$ that the calculated values of the mutual polarizabilities between the ligand tin(II) atoms (vide infra) were quite similar. With regard to the Slater exponent and the ionization potential of the valence atomic orbital for the other atoms, the reported values were adopted.[11]

According to Pople and Santry,[12] the nuclear spin–spin coupling constant is given by eq 1 and 2, as far as the Fermi contact interaction

$$J(\mathrm{AB}) = (16h\beta^2/9)\gamma_\mathrm{A}\gamma_\mathrm{B}[s_\mathrm{A}(0)]^2[s_\mathrm{B}(0)]^2\pi(\mathrm{AB}) \qquad (1)$$

$$\pi(\mathrm{AB}) = -4\sum_{i}^{\mathrm{occ}}\sum_{j}^{\mathrm{unocc}}(\epsilon_i - \epsilon_j)^{-1}C_{i\mathrm{A(s)}}C_{j\mathrm{A(s)}}C_{i\mathrm{B(s)}}C_{j\mathrm{B(s)}} \qquad (2)$$

dominates the coupling mechanism. Here γ is the gyromagnetic ratio, β is the Bohr magneton, $[s(0)]^2$ is the valence s orbital electron density of an atom at the nucleus, and $\pi(\mathrm{AB})$ is the mutual polarizability of the valence s orbitals of atom A and B; the ϵ's are orbital energies, and C's are orbital coefficients.

By comparing observed $^2J(\mathrm{SnSn})$ with calculated $^2\pi(\mathrm{SnSn})$ in eq 1, it is possible to evaluate the $[s(0)]^2$ values in the coordinated tin atoms. As summarized in Table I, the extended Hückel molecular orbital treatments gave magnitudes in satisfactory agreement with the SCF value (15.3 au), which was estimated by extrapolating the reported SCF values of the oxidation states (−I, 0, I).[13] Pertinence of the present Pople–

---

(2) With respect to tin(II)-coordinated transition-metal complexes, see: (a) Moriyama, H.; Aoki, T.; Shinoda, S.; Saito, Y. *J. Chem. Soc., Chem. Commun.* **1982**, 500. (b) Farrugia, L. J.; James, B. R.; Lassigne, C. R.; Wells, E. J. *Can. J. Chem.* **1982**, *60*, 1304. (c) Moriyama, H.; Pregosin, P. S.; Saito, Y.; Yamakawa, T. *J. Chem. Soc. Dalton Trans.* **1984**, 2329. (d) Moriyama, H.; Aoki, T.; Shinoda, S.; Saito, Y. *J. Chem. Soc., Dalton Trans* **1981**, 639. (e) Yamakawa, T.; Shinoda, S.; Saito, Y.; Moriyama, H.; Pregosin, P. S. *Magn. Reson. Chem.* **1985**, *23*, 202. (f) Nelson, J. H.; Alcock, N. W. *Inorg. Chem.* **1982**, *21*, 1196. (g) Alcock, N. W.; Nelson, J. H. *J. Chem. Soc., Dalton Trans.* **1982**, 245. (h) Pregosin, P. S.; Rüegger, H. *Inorg. Chim. Acta* **1984**, *86*, 55.

(3) Pidcock, A.; Heaton, B. T. *J. Organomet. Chem.* **1968**, *14*, 235. Grim, S. O.; Wheatland, D. A. *Inorg. Nucl. Chem. Lett.* **1968**, *4*, 187. Allen, F. H.; Sze, S. N. *J. Chem. Soc. A* **1971**, 2054. Clark, H. C.; Manzer, L. E. *Inorg. Chem.* **1972**, *11*, 2749. Chatt, J.; Mason, R.; Meek, D. W. *J. Am. Chem. Soc.* **1975**, *97*, 3826. Miyamoto, T. *J. Organomet. Chem.* **1977**, *134*, 335. Appleton, T. G.; Bennett, M. A. *Inorg. Chem.* **1978**, *17*, 738. Carius, M. A.; Dixon, K. R.; Rivett, G. A. *J. Organomet. Chem.* **1979**, *171*, 373. Motschi, H.; Pregosin, P. S. *Inorg. Chim. Acta* **1980**, *40*, 141. Koie, Y.; Shinoda, S.; Saito, Y. *J. Chem. Soc., Dalton Trans.* **1981**, 1082. Anderson, A.; Clark, H. C.; Davis, J. A. *Inorg. Chem.* **1981**, *20*, 1636. Albinati, A.; Gunten, U. V.; Pregosin, P. S.; Rüegger, H. J. *J. Organomet. Chem.* **1985**, *295*, 239. Blau, R. J.; Esperson, H. O. *Inorg. Chem.* **1986**, *25*, 878.

(4) McFarlane, W. *Q. Rev., Chem. Soc.* **1969**, *23*, 187. Murrell, J. N. *Progr. Nucl. Magn. Reson. Spectrosc.* **1971**, *6*, 1.

(5) Shaw, B. L.; Powell, J. J. *J. Chem. Soc.* **1962**, 5075. Powell, J.; Shaw, B. L. *Ibid.* **1965**, 3879. Pidcock, A.; Richards, R. E.; Venanzi, L. M. *J. Chem. Soc. A* **1966**, 1707. Allen, F. H.; Pidcock, A. *Ibid.* **1968**, 2700. Church, M. J.; Mays, N. J. *Ibid.* **1968**, 3074; **1970**, 8. Mather, G. G.; Pidcock, A. *Ibid.* **1970**, 1226. Bennett, J.; Pidcock, A.; Waterhouse, C. R.; Coggau, P.; McPhail. A. T. *Ibid.* **1970**, 2094. Chisholm, M. H.; Clark, H. C.; Manzer, L. E.; Stothers, J. B. *J. Chem. Soc. D* **1971**, 1627. Henneike, H. F. *J. Am. Chem. Soc.* **1972**, *94*, 5945. Pregosin, P. S.; Omura, H.; Venanzi, L. E. *Ibid.* **1973**, *95*, 2047. Chisholm, M. H.; Clark, H. C.; Manzer, L. E.; Stothers, J. B.; Ward, J. E. H. *Ibid.* **1973**, *95*, 8574. Cherwinski, W. J.; Johnson, B. F. G.; Lewis, *J. Chem. Soc., Dalton Trans.* **1975**, 1156. Dixon, K. R.; Moss, K. C.; Smith, M. A. R. *Ibid.* **1975**, 990. Iwayanagi, T.; Saito, Y. *Inorg. Nucl. Chem. Lett.* **1975**, *11*, 459. Iwayanagi, T.; Ibusuki, T.; Saito, Y. *J. Organomet. Chem.* **1977**, *128*, 145. Motschi, H.; Pregosin, P. S.; Venanzi, L. M. *Helv. Chim. Acta* **1979**, *62*, 667. Koie, Y.; Shinoda, S.; Saito, Y. *Inorg. Chem.* **1981**, *20*, 4408. Kerrison, S. J. S.; Sadler, P. J. *J. Chem. Soc., Chem. Commun.* **1982**, 2363.

(6) Appleton, T. G.; Hall, J. R.; Ralph, S. F. *Inorg. Chem.* **1985**, *24*, 4685.

(7) Schenk, W. A.; Buchner, W. *Inorg. Chim. Acta* **1983**, *70*, 189. Buchner, W.; Schenk, W. A. *Inorg. Chem.* **1984**, *23*, 132.

(8) Wolfsberg, M.; Helmholtz, L. *J. Chem. Phys.* **1952**, *20*, 837.

(9) Yurchenko, E. N.; Devyatkira, E. T.; Khodashova, T. S.; Porai-Koshits, M. A.; Konnov, V. I.; Vernek, V. A.; Antonov, P. G.; Kukushikin, Yu. N. *Koord. Khim.* **1979**, *5*, 552.

(10) Muir, K. W.; Ibers, J. A. *Inorg. Chem.* **1970**, *9*, 440. Manojlovic-Muir, L.; Muir, K. W. *Ibid.* **1970**, *9*, 447.

(11) Basch, H.; Gray, H. B. *Theor. Chim. Acta* **1966**, *4*, 367. Thorn, D. L.; Hoffmann, R. *Inorg. Chem.* **1978**, *17*, 126. Berke, H.; Hoffmann, R. *J. Am. Chem. Soc.* **1978**, *100*, 7224. Silvestre, J.; Albright, T. A.; Sosinsky, B. A. *Inorg. Chem.* **1981**, *20*, 3937. Evans, D. G.; Mingos, D. M. P. *Organometallics* **1983**, *2*, 435.

(12) Pople, J. A.; Santry, P. D. *Mol. Phys.* **1964**, *8*, 1.

Santry approximation for these tin(II)-coordinated complexes is well demonstrated for the complexes coordinated with chemically equivalent but magnetically nonequivalent ligand atoms (vide post).

Results and Discussion

(1) EHMO Interpretation of Ligand–Ligand Coupling Constants of Square-Planar Platinum(II) Complexes. The geminal phosphorus–phosphorus nuclear spin coupling constants of transition-metal complexes, coordinated with phosphine ligands, exhibit generally the following trends:[14] (i) the magnitude is larger for $^2J(PP)_{trans}$ than for $^2J(PP)_{cis}$, and (ii) the sign is positive for $^2J(PP)_{trans}$ but negative for $^2J(PP)_{cis}$. An EHMO interpretation was given previously for $[PtCl(PMe_3)_3]^+$ from the viewpoint of the molecular symmetry and the participation of metal p and d orbitals in coordination.[15] A high-lying occupied MO of strongly donating Pt(p)-type coordination was responsible for $^2J(PP)_{trans}$, whereas a low-lying occupied MO of weakly donating Pt(d)-type coordination was important for $^2J(PP)_{cis}$. It is worthwhile to mention that the large participation of the metal p orbital in coordination brings about the positive large nuclear spin coupling constant for the trans-disposed phosphorus atoms as well as the small magnitude for cis coupling.

As pointed out recently by Pregosin et al.,[2h] the geminal tin–tin nuclear spin coupling constants of the tin(II)-coordinated platinum(II) square-planar complexes, cis-$[PtCl_2(SnCl_3)_2]^{2-}$, $[PtCl(SnCl_3)_3]^{2-}$, and $[Pt(SnCl_3)_4]^{2-}$, exhibit the order of $|^2J(SnSn)_{trans}| > |^2J(SnSn)_{cis}|$ similar to trend i for $^2J(PP)$. The magnitudes of the geminal nuclear spin coupling constants, $^2J(SnSn)$, and the corresponding ones, $^2K(SnSn)$, were summarized in Table II for these tin(II)-coordinated complexes, together with those of $[PtCl(PMe_3)_3]^+$, the signs and magnitudes of which were well interpreted by the EHMO method.[15] The signs of the nuclear spin coupling constants are able to be predicted with the calculated mutual polarizabilities between the valence s orbitals of the spin-coupled atoms from eq 1. In the case of $[IrH(SnCl_3)_5]^{3-}$, the observed opposite relationship in sign between $^2J(Sn_{ax}H)_{trans}$ and $^2J(Sn_{eq}H)_{cis}$ was well reproduced in terms of the calculated mutual polarizabilities.[16]

Since the magnetic dipole moments of the magnetically active ($I = {}^1/_2$) tin nuclei, ^{119}Sn and ^{117}Sn, are negative (-9.97146×10^7 and -9.53080×10^7 rad T^{-1} s^{-1}, respectively), $^2J(SnSn)$ and $^2\pi(SnSn)$ possess the same sign. The values of $^2\pi(SnSn)_{trans}$ and $^2\pi(SnSn)_{cis}$ for the tin(II)-coordinated complexes, included in Table II, were positive and negative in sign, respectively. A prediction could be made, therefore, for the signs of $^2J(SnSn)_{trans}$ and $^2J(SnSn)_{cis}$ to be positive and negative, respectively. Their signs are consequently corresponding to those of $^2J(PP)$ (trend ii).

The tendency for the observed magnitude of $^2J(SnSn)$ to be larger for trans than for cis was reproduced for all of these complexes in $^2\pi(SnSn)$ as $|^2\pi(SnSn)_{trans}| > |^2\pi(SnSn)_{cis}|$. The large difference of $|^2K(SnSn)| > |^2K(PP)|$ (e.g., $^2K(SnSn)_{trans} = 2740 \times 10^{21}$ cm^{-3} for $[PtCl(SnCl_3)_3]^{2-}$ vs. $^2K(PP)_{cis} = 21.0 \times 10^{21}$ cm^{-3} for $[PtCl(PMe_3)_3]^+$) seems to be ascribed to the coordination properties rather than the atomic difference in the $[s(0)]^2$ term (15.3 for tin and 7.61 for phosphorus, respectively[13]).

Not only the signs but also the magnitudes of the nuclear spin coupling constants are thus well interpreted for metal complexes by the Pople–Santry approach within the EHMO framework.

(2) Characterization of Constituent Molecular Orbitals Responsible for Tin–Tin Spin Coupling Constants in $[Ru(SnCl_3)_6]^{4-}$.

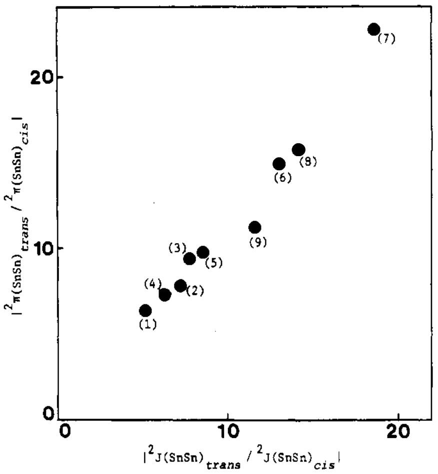

Figure 1. Correlation of the observed geminal tin–tin coupling constants with the calculated mutual polarizabilities in the trans-to-cis ratio for tin(II)-coordinated octahedral metal complexes: (1) $[Ru(SnCl_3)_6]^{4-}$; (2) $[RuCl(SnCl_3)_5]^{4-}$; (3) *trans*-$[RuCl_2(SnCl_3)_4]^{4-}$; (4) $[Os(SnCl_3)_6]^{4-}$; (5) $[OsCl(SnCl_3)_5]^{4-}$; (6) $[RhH(SnCl_3)_5]^{3-}$; (7) *trans*-$[IrCl_2(SnCl_3)_4]^{3-}$; (8) *trans*-$[IrClH(SnCl_3)_4]^{3-}$; (9) $[IrH(SnCl_3)_5]^{3-}$.

Table III. Observed Geminal Tin–Tin Coupling Constants and Corresponding Mutual Polarizabilities of Tin(II)-Coordinated Transition-Metal Complexes

	$^2J(SnSn)^a$/Hz		$^2\pi(SnSn)$/ 10^{-3} eV^{-1}	
complex	trans	cis	trans	cis
$[Ru(SnCl_3)_6]^{4-}$	13034	2429	+4.78	−0.77
$[RuCl(SnCl_3)_5]^{4-}$	21254	2938	+6.18	−0.79
trans-$[RuCl_2(SnCl_3)_4]^{4-}$	26914	3455	+8.12	−0.86
$[Os(SnCl_3)_6]^{4-}$	11250	1775	+4.12	−0.57
$[OsCl(SnCl_3)_5]^{4-}$	18600	2169	+5.60	−0.57
$[RhH(SnCl_3)_5]^{3-}$	25506	1975	+6.67	−0.44
$[IrH(SnCl_3)_5]^{3-}$	21094	1820	+5.91	−0.53
trans-$[IrClH(SnCl_3)_4]^{3-}$	30225	2145	+8.09	−0.51
trans-$[IrCl_2(SnCl_3)_4]^{3-}$	37672	2025	+9.91	−0.44

[a] Signs undetermined for the nuclear spin coupling constants of tin(II)-coordinated complexes.

The octahedral complexes with four equatorial tin(II) ligand atoms are particularly important in the present approach for the following reasons: (i) the $[s(0)]^2$ terms canceled each other because of the chemical equivalency, as far as the two kinds of geminal tin–tin nuclear spin coupling constants are treated in ratio, $|^2J(SnSn)_{trans}/^2J(SnSn)_{cis}|$. (ii) The spin–spin coupling constants in coordination are able to be examined through the selected molecular orbitals, for which the valence s orbital mutual polarizabilities between the equatorial ligand atoms are responsible. (iii) Even in the complexes of magnetically nonactive metal species, the two-bond ($\underline{Sn}$–M–$\underline{Sn}$) coupling constants are well elucidated by the present approach, while the one-bond ($\underline{M}$–$\underline{Sn}$) nuclear spin coupling information is added for the magnetically active metallic species. (iv) A cis influence on the tin equatorial ligands can be investigated for various axial ligands.

In the Pople–Santry approximation, the observed ratios $|^2J(SnSn)_{trans}/^2J(SnSn)_{cis}|$ must be proportional to the calculated ratios $|^2\pi(SnSn)_{trans}/^2\pi(SnSn)_{cis}|$ in the series of the octahedral complexes with four equatorial tin(II) ligand atoms, since the term of the valence s orbital electron density, $[s(0)]^2$, is canceled because of the chemical equivalency among the equatorial tin(II) ligand atoms. An excellent linear relationship, passing through the origin, was obtained as expected for the various kinds of complexes reported so far (Figure 1). The Pople–Santry approximation is therefore satisfactorily applicable to the tin(II)-coordinated octahedral metal complexes. The general trends of $|^2J(SnSn)_{trans}|$ and $|^2\pi(SnSn)_{trans}|$ being larger than $|^2J(SnSn)_{cis}|$ and $|^2\pi(SnSn)_{cis}|$, respectively, were confirmed for all of these complexes (Table III).

In order to understand the geminal tin–tin spin coupling constants in more detail, the molecular orbital analysis relevant to

---

(13) Kunz, R. W. *Helv. Chim. Acta* **1980**, *63*, 2054.

(14) Nixon, J. F.; Pidcock, A. *Annu. Rev. NMR Spectrosc.* **1969**, *2*, 345.

(15) Koie, Y.; Shinoda, S.; Saito, Y. *Inorg. Nucl. Chem. Lett.* **1981**, *17*, 147.

(16) The ^{119}Sn NMR spectrum of $[IrH(SnCl_3)_5]^{3-}$ shows the ABX spectrum pattern, where A or B is the axial or equatorial ^{119}Sn nucleus and X is the ligand ^1H nucleus, respectively. The magnitudes of the geminal spin coupling constants were $|^2J(Sn_{ax}H)_{trans} + {}^2J(Sn_{eq}H)_{cis}| = 781.3$ Hz for ABX, $|^2J(Sn_{ax}H)_{trans}| = 864.3$ Hz for AX, and $|^2J(Sn_{eq}H)_{cis}| = 83.0$ Hz for BX spectrum patterns, respectively. These values for the signs of $^2J(SnH)_{trans}$ and $^2J(SnH)_{cis}$ have to be opposite. Actually, the sign of $^2\pi(SnH)_{trans}$ (7.24×10^{-3} eV^{-1}) was calculated to be opposite to that of $^2\pi(SnH)_{cis}$ (-2.54×10^{-3} eV^{-1}).

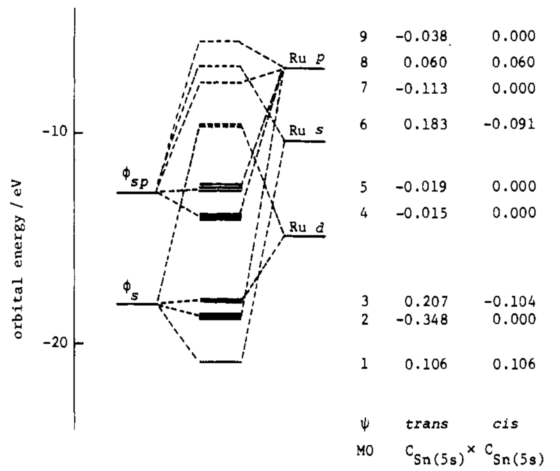

Figure 2. Orbital interaction diagram for $[Ru(SnCl_3)_6]^{4-}$ molecular orbitals constituted from the Ru, s, p, and d orbitals and the ligand s and sp σ orbitals with the valence s orbital coefficient products.

$^2\pi$(SnSn) in the d^6 metal complex with four equatorial tin(II) ligands has been accomplished. The first example is $[Ru(SnCl_3)_6]^{4-}$ of O_h symmetry.

In Figure 2, an orbital-interaction diagram is depicted for $[Ru(SnCl_3)_6]^{4-}$, made from the ruthenium s, p, and d orbitals and the fragment orbitals of the $SnCl_3^-$ ligand. The values of the valence s orbital coefficient products are added for the enrolled molecular orbitals, where the trans- and cis-disposed tin ligand atoms make a large contribution of $(C_{Sn(5s)}C_{Sn(5s)})_{trans}$ and $(C_{Sn(5s)}C_{Sn(5s)})_{cis}$, respectively. There are two occupied molecular orbitals for the $SnCl_3^-$ fragment extending to the σ coordinate with the ruthenium atom; one is the s type orbital, ϕ_s (**1**, $\epsilon = -18.11$ eV), and the other sp type, ϕ_{sp} (**2**, $\epsilon = -12.92$ eV). With regard to the molecular orbitals dominated by the ruthenium p orbital, the cis-disposed tin ligand atoms receive no share because of the orbital symmetry. The molecular orbitals ψ_2, ψ_4, ψ_5, ψ_7, and ψ_9 belong to this category.

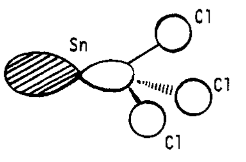

(1)

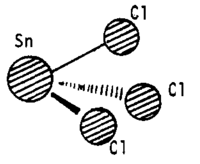

(2)

First, the trans-disposed tin–tin coupling constants will be dealt with. Let us examine low-lying molecular orbitals ψ_1 (**3**), ψ_2 (**4**), and ψ_3 (**5**), which are composed of the low-lying Sn(II) filled s orbital, ϕ_s, σ-donating to the vacant Ru(II) s, p, and d orbitals with single, triple, and double degeneration, respectively. As for the contributions to the trans-disposed geminal tin–tin spin coupling constant, the contribution from both ψ_1 (**3**) and ψ_3 (**5**) with positive valence s orbital coefficient products of 0.106 and 0.207, respectively, were almost canceled by the one from ψ_2 (**4**) with the negative products (−0.348).

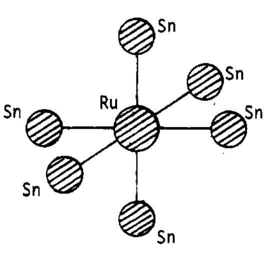

(3)

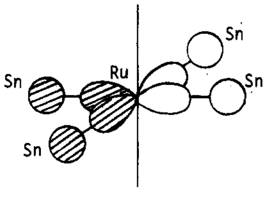

(4)

The high-lying occupied molecular orbitals ψ_4 and ψ_5 (**6**) (HOMO, $\epsilon = -12.58$ eV) are composed of the high-lying Sn(II) filled sp orbital, ϕ_{sp}, σ-donating to the triply degenerate vacant Ru(II) p orbital. On the contrary, the Ru(II) filled d orbitals afforded unoccupied molecular orbitals; a triply degenerated vacant molecular orbital (LUMO, $\epsilon = -9.84$ eV), consisting of the Ru dσ–Sn pσ interaction, is lacking the contribution of the Sn s orbital, whereas the relatively low unoccupied molecular orbitals of doubly degenerate ψ_{6a} (**7**) and ψ_{6b} (**8**) (secondary LUMO, $\epsilon = -9.52$ eV) are made from the antibonding Ru dσ–Sn ϕ_s coordination.

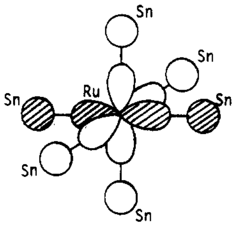

(5)

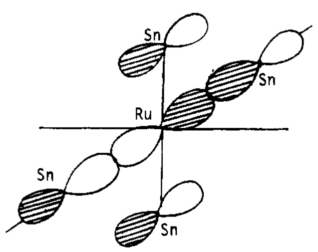

(6)

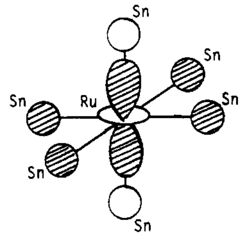

(7)

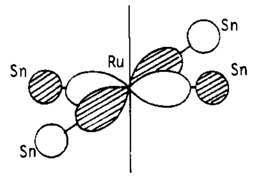

(8)

The mutual polarizability between the valence s orbitals of the spin-coupled atoms is determined by the following two factors; one is the energy separation between the occupied and the unoccupied molecular orbitals containing the valence s orbital coefficients concerned, $\epsilon_i - \epsilon_j$, and the other is the magnitude of the double product of the valence s orbital coefficients of the spin-coupled atoms in both the occupied and unoccupied molecular orbitals, $C_{i\mathrm{Sn(s)}}C_{i\mathrm{Sn'(s)}}C_{j\mathrm{Sn(s)}}C_{j\mathrm{Sn'(s)}}$. For this reason, the predominantly large magnitude of the double product, coupled with the small energy separation, will make a dominant contribution to the mutual polarizability. In the case of the trans-disposed tin ligand atoms of $[Ru(SnCl_3)_6]^{4-}$, the contribution of a set of the occupied and unoccupied molecular orbitals, i.e., the transition from ψ_5 (**6**) to ψ_6 (**7** and **8**), amounted to 95% of $^2\pi(\mathrm{SnSn})_{trans}$. This type of predominance of a certain important pair of the occupied and unoccupied molecular orbitals for determining the nuclear spin coupling constants was previously treated as the ΔE approximation.[17] Although the sign of spin coupling constants is unpredictable by the ΔE approximation, a positive sign is deduced for $^2J(\mathrm{SnSn})_{trans}$ on the basis of the s orbital coefficient double products of ψ_5(**6**) and ψ_6 (**7** and **8**).

The metal p orbital is not responsible for $^2J(\mathrm{SnSn})_{cis}$ for the symmetry reason, in contrast to the s and d orbitals. The metal s orbital requires the same sign for the cis-ligand s orbitals, whereas the metal d orbital results in a different sign, as shown in ψ_1 (**3**) and ψ_3 (**5**). Their contributions to $^2\pi(\mathrm{SnSn})_{cis}$ are canceled with each other because of the opposite sign of the s orbital coefficient products. The same sort of cancellation is found for the unoccupied ψ_6 (**7** and **8**) and ψ_8 (**9**) molecular orbitals, which are also composed of the metal d and s orbitals, respectively. These competing features due to the orbital symmetry certainly decrease the magnitude of $^2J(\mathrm{SnSn})_{cis}$ in contrast to the sole and large contribution of the metal p orbital to $^2J(\mathrm{SnSn})_{trans}$.

Consequently, the observed tendencies $^2J(\mathrm{SnSn})_{trans} > 0$ and $|^2J(\mathrm{SnSn})_{trans}| > |^2J(\mathrm{SnSn})_{cis}|$ in $[Ru(SnCl_3)_6]^{4-}$ were reasonably understood in terms of MO characteristics.

(3) Molecular Orbitals of *trans*-$[RuCl_2(SnCl_3)_4]^{4-}$ Responsible for Tin–Tin Spin Coupling Constants. Figure 3 shows the MO

---

(17) McConnell, H. M. *J. Chem. Phys.* **1965**, *24*, 460.

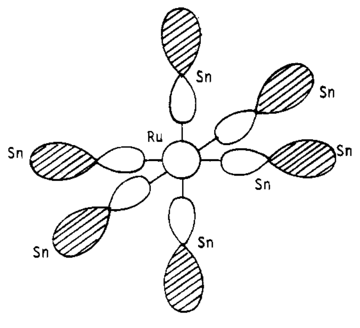

(9)

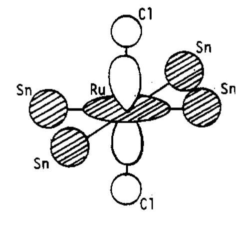

(10)

characteristics of *trans*-[RuCl$_2$(SnCl$_3$)$_4$]$^{4-}$, where the citation of molecular orbitals is limited to those with nonzero s orbital coefficients concerning the trans- or cis-disposed tin ligand atoms.

The lowest-lying molecular orbital of ψ'_1 (**10**) is composed of the s orbitals of the ligand tin and chlorine atoms together with the metal s and d$_{z^2}$ orbitals. In the occupied molecular orbitals of ψ'_2 (**11**) and ψ'_3 (**12**), the doubly degenerate metal p orbital and the d$_{x^2-y^2}$ orbital are used for the coordination with the equatorial tin ligand atoms, respectively. Due to the symmetry of the metal s and d orbitals, the trans-disposed valence s orbital coefficient products are positive for the molecular orbitals of ψ'_1 (**10**) and ψ'_3 (**12**) (0.163 and 0.155, respectively), whereas that of ψ'_2 (**11**) is negative (−0.354) on account of the p-type orbital symmetry. They almost canceled each other in a manner similar to that encountered for [Ru(SnCl$_3$)$_6$]$^{4-}$. Analogous to its ψ_1 (**3**), ψ_2 (**4**), and ψ_3 (**5**) orbitals, the ψ'_1 (**10**), ψ'_2 (**11**), and ψ'_3 (**12**) orbitals are all composed of the low-lying filled Sn(II) s orbital, ϕ_s, σ-donating to the Ru(II) vacant s, p, and d orbitals, respectively.

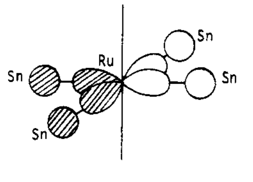

(11)

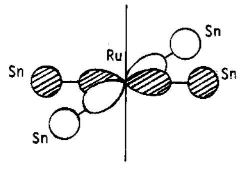

(12)

The high-lying occupied molecular orbitals ψ'_4 and ψ'_5 (**13**) (HOMO, $\epsilon = -12.52$ eV) are mainly composed of the tin ligand ϕ_{sp} orbital, σ-donating to the doubly degenerate Ru(II) vacant p orbital. The unoccupied molecular orbital, ψ'_6 (**14**) (LUMO, $\epsilon = -10.00$ eV), is antibonding with respect to the ruthenium d$_{z^2}$ orbital and the axially-coordinated chlorine sp-hybridized orbital in addition to a small repulsive contribution due to the tin s orbital. On the other hand, the unoccupied molecular orbital ψ'_7 (**15**) is antibonding with respect to the ruthenium d$_{x^2-y^2}$ and tin s orbitals.

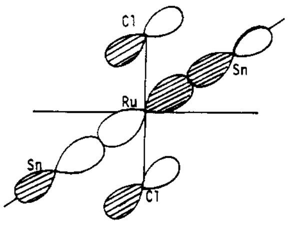

(13)

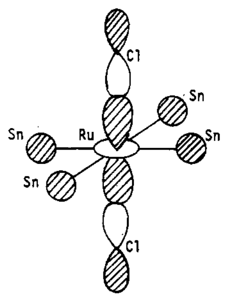

(14)

Because of the small energy separation and the large magnitude of the s coefficient double products, the transitions from ψ'_5 (**13**) to both ψ'_6 (**14**) and ψ'_7 (**15**) were ascertained to make a major contribution, amounting to 97% of the $^2\pi$(SnSn)$_{trans}$ value.

The molecular orbitals ψ'_2, ψ'_4, ψ'_5, ψ'_8, and ψ'_{10} are all composed of the ruthenium p orbitals, which give no contribution to (C$_{Sn(5s)}$C$_{Sn(5s)}$)$_{cis}$ because of the orbital symmetry. On the contrary, the molecular orbitals, composed of the ruthenium s and/or d orbitals, i.e., ψ'_1, ψ'_3, ψ'_6, ψ'_7, and ψ'_9, contribute to $^2\pi$(SnSn)$_{cis}$. On account of the aforementioned cancellation, between the metal s and d orbitals, *trans*-[RuCl$_2$(SnCl$_3$)$_4$]$^{4-}$ gave the order $|^2J$(SnSn)$_{trans}| > |^2J$(SnSn)$_{cis}|$, as expected from [Ru(SnCl$_3$)$_6$]$^{4-}$.

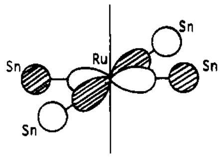

(15)

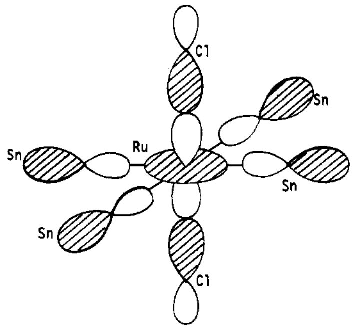

(16)

(4) Cis Influence of the Axial Ligand on Tin–Tin Spin Coupling Constants. It is worthwhile to mention that both $^2\pi$(SnSn)$_{trans}$ (8.12×10^{-3} eV^{-1}) and ^2J(SnSn)$_{trans}$ (26 914 Hz) are larger for *trans*-[RuCl$_2$(SnCl$_3$)$_4$]$^{4-}$ than for [Ru(SnCl$_3$)$_6$]$^{4-}$ (4.78×10^{-3} eV^{-1} and 13 034 Hz, respectively). In this aspect, the magnitude of ^2J(SnSn)$_{trans}$ is an important index of the cis influence exerted by the axial ligands.

As noted in the previous sections, a certain set of a high-lying occupied molecular orbital and a low-lying unoccupied one substantially determines the magnitude of the nuclear spin coupling between the trans-disposed ligand atoms. The largest contribution to ^2J(SnSn)$_{trans}$ among the occupied molecular orbitals was made by ψ_5 (**6**) for [Ru(SnCl$_3$)$_6$]$^{4-}$ and by ψ'_5 (**13**) for *trans*-[RuCl$_2$(SnCl$_3$)$_4$]$^{4-}$, both of which are the HOMO with large valence s coefficient double products. They are close in energy to each other (−12.58 eV for ψ_5 (**6**) and −12.52 eV for ψ'_5 (**13**)).

The role of the unoccupied ruthenium d orbital in the ψ_{6a} (**7**) of [Ru(SnCl$_3$)$_6$]$^{4-}$ or ψ'_6 (**14**) of *trans*-[RuCl$_2$(SnCl$_3$)$_4$]$^{4-}$ seems to be especially important for the cis influence of the axial ligand atoms, tin or chlorine.

In Figure 4, the schematic orbital interactions for these complexes are illustrated with the ruthenium dσ orbitals (d$_{z^2}$ and d$_{x^2-y^2}$) and the ligand orbitals (SnCl$_3^-$ (ϕ_s) and Cl$^-$ (s and p)). The doubly degenerate unoccupied Ru(II) dσ orbitals in ψ_6 (**7** and **8**) of [Ru(SnCl$_3$)$_6$]$^{4-}$ were split by the axial ligand substitution with chloride into the ψ'_6 (**14**) and ψ'_7 (**15**) orbitals of *trans*-[RuCl$_2$(SnCl$_3$)$_4$]$^{4-}$. The ψ'_6 (**14**) orbital is mainly composed of the ruthenium d$_{z^2}$ orbital and the s and p orbitals of the chloride ligands, whereas the ψ'_7 (**15**) orbital, similar to ψ_{6b} (**8**) of [Ru(SnCl$_3$)$_6$]$^{4-}$, is mainly composed of the ruthenium d$_{x^2-y^2}$ orbital and the tin ligand ϕ_s orbitals. As expected, the energy level of ψ'_7 (**15**) (−9.51 eV) was almost the same as that of ψ_6 (**7** and **8**) (−9.52 eV). On the contrary, the energy level of ψ_6 (**14**) (−10.00 eV) became lower than that of ψ'_7 (**15**) (−9.51 eV), because the degenerated orbital ψ_6 (**7** and **8**) was split by the perturbation of the axial chloride ligand, endowed with relatively deep valence state ionization potentials (VSIP) of Cl (−26.3 eV for 2s and −14.2 eV for 2p of Cl in contrast to −18.11 eV for ϕ_s and −12.92 eV for ϕ_{sp} of SnCl$_3^-$).

The transitions of ψ'_5 (**13**) → ψ'_6 (**14**) (1.89×10^{-3} eV^{-1}) and ψ'_5 (**13**) → ψ'_7 (**15**) (6.00×10^{-3} eV^{-1}) constituted ^2J(SnSn)$_{trans}$ (26 914 Hz) predominantly in *trans*-[RuCl$_2$(SnCl$_3$)$_4$]$^{4-}$, whereas the degenerated transition of ψ_5 (**6**) → ψ_{6a} (**7**) and ψ_5 (**6**) → ψ_{6b} (**8**) (4.54×10^{-3} eV^{-1}) in [Ru(SnCl$_3$)$_6$]$^{4-}$ determined ^2J(SnSn)$_{trans}$ (13 034 Hz) almost solely. The cis influence on ^2J(SnSn)$_{trans}$ of the axial chloride ligands is consequently ascribed to the energy splitting induced by the orbital perturbation of the axial Cl$^-$ ligand, which has a lower energy level than the SnCl$_3^-$ ligand.

As summarized in Table III, the values of ^2J(SnSn)$_{trans}$ in the series of *trans*-[MLL′(SnCl$_3$)$_4$]$^{n-}$ complexes are quite sensitive to the axial ligands, with a common influence on both ^2J(SnSn)$_{trans}$ and $^2\pi$(SnSn)$_{trans}$ exerted by the axial ligand substitution.

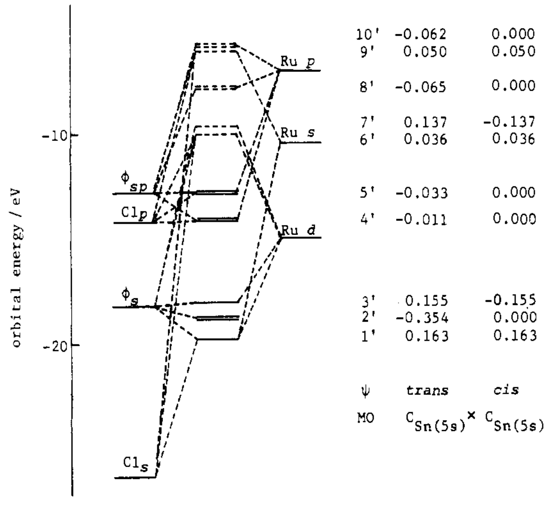

Figure 3. Orbital interaction diagram for *trans*-$[RuCl_2(SnCl_3)_4]^{4-}$ molecular orbitals constituted from the Ru, s, p, and d orbitals and the ligand orbitals with the valence s orbital coefficient products.

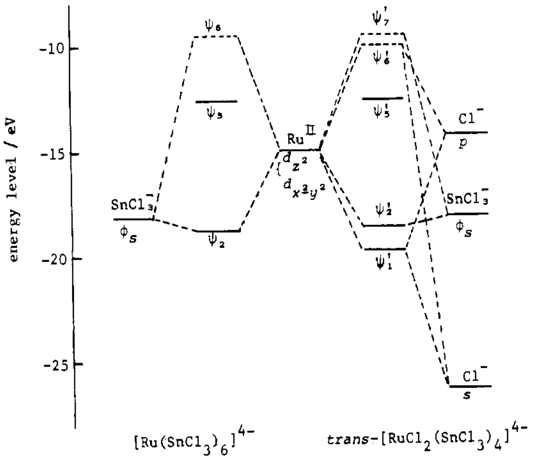

Figure 4. Selected orbital interactions to compare $[Ru(SnCl_3)_6]^{4-}$ and *trans*-$[RuCl_2(SnCl_3)_4]^{4-}$ molecular orbitals constituted from Ru $d\sigma$ orbitals and the axial ligand s and p orbitals.

In good accord with the difference between $[Ru(SnCl_3)_6]^{4-}$ and *trans*-$[RuCl_2(SnCl_3)_4]^{4-}$, larger values were induced for ${}^2J(SnSn)_{trans}$ and ${}^2\pi(SnSn)_{trans}$ by the axial chloride ligand, as ascertained for the set $[IrH(SnCl_3)_5]^{3-}$, *trans*-$[IrClH(SnCl_3)_4]^{3-}$, and *trans*-$[IrCl_2(SnCl_3)_4]^{3-}$. The role of an axial hydride ligand became apparent, since ${}^2J(SnSn)_{trans}$ (21 094 → 30 225 → 37 672 Hz in this order) and ${}^2\pi(SnSn)_{trans}$ ($5.91 \times 10^{-3} \rightarrow 8.09 \times 10^{-3} \rightarrow 9.91 \times 10^{-3}$ eV^{-1}) varied correspondingly for the series $[IrH(SnCl_3)_5]^{3-}$, *trans*-$[IrClH(SnCl_3)_4]^{3-}$ and *trans*-$[IrCl_2(SnCl_3)_4]^{3-}$ complexes. In these iridium complexes, the transitions from the HOMO to both the LUMO and the secondary LUMO were important for determining the values of ${}^2\pi(SnSn)_{trans}$ in the similar situation with *trans*-$[RuCl_2(SnCl_3)_4]^{4-}$. Among the above-mentioned molecular orbitals, only the LUMO was sensitive to the axial ligands, since this orbital was constituted with the iridium s and d_{z^2} orbitals, the equatorial tin ϕ_s orbitals, and the donating orbital of the axially coordinated ligand atoms. On the contrary, either the HOMO, composed of the iridium p orbital, or the secondary LUMO, composed of the iridium $d_{x^2-y^2}$ orbital, was indifferent to the axial ligand atoms because of the orbital symmetry. As pointed out previously, the small transition energy is important for determining the magnitude of either π or J of the trans-disposed equatorial tin ligand atoms. For this reason, attention must be paid to the energy level of the LUMO from the viewpoint of cis influence.

The energy level of the LUMO was lower for *trans*-$[IrCl_2(SnCl_3)_4]^{3-}$ (−11.66 eV) than for *trans*-$[IrClH(SnCl_3)_4]^{3-}$ (−11.33 eV). Since chlorine has deeper VSIP values (2p, −14.2 eV; 2s, −26.3 eV) than hydrogen (1s, −13.6 eV), the energy level of LUMO is again closely related to the VSIP values of the axial ligand atoms. The key to understanding the cis influence on ${}^2J(SnSn)_{trans}$ is afforded, therefore, by the interaction between the iridium d_{z^2} orbital and the σ-donating orbital of the axially coordinated atoms through their VSIP values.

Table IV. Observed Metal–Tin Ligand One-Bond Coupling Constants and Corresponding Mutual Polarizabilities of Tin(II)-Coordinated Ruthenium and Osmium Complexes

complex	${}^1J(MSn_{eq})^a$/Hz	${}^1\pi(MSn_{eq})/10^{-3}$ eV^{-1}
$[Ru(SnCl_3)_6]^{4-}$	756	+1.43
$[RuCl(SnCl_3)_5]^{4-}$	846	+1.92
trans-$[RuCl_2(SnCl_3)_4]^{4-}$	1123	+2.58
$[Os(SnCl_3)_6]^{4-}$	1123	+0.96
$[OsCl(SnCl_3)_5]^{4-}$	1290	+1.36

[a] Signs undetermined for the nuclear spin coupling constants in tin(II)-coordinated complexes.

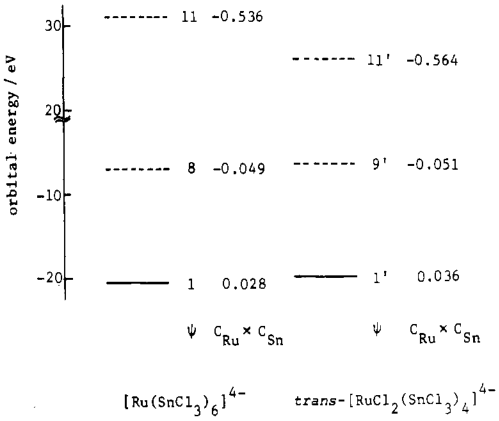

Figure 5. Occupied and unoccupied molecular orbitals important for determining ${}^1J(SnRu)$ values of $[Ru(SnCl_3)_6]^{4-}$ and *trans*-$[RuCl_2(SnCl_3)_4]^{4-}$ with the valence s orbital coefficient products.

(5) Cis Influence on Metal–Tin Direct Coupling Constants. The observed one-bond coupling constants and the corresponding mutual polarizabilities between the metal atom and the tin atom in the equatorial position were listed in Table IV for the magnetically active ruthenium and osmium complexes (${}^{99}Ru$, $I = {}^5/_2$, NA (natural abundance) = 12.72%; ${}^{187}Os$, $I = {}^1/_2$, NA = 1.64%). Evidently, they are sensitive to the axial ligands.

In Figure 5, the important molecular orbitals are depicted for the two kinds of the tin(II)-coordinated ruthenium complexes, $[Ru(SnCl_3)_6]^{4-}$ and *trans*-$[RuCl_2(SnCl_3)_4]^{4-}$, in which the valence s orbital coefficient products of ruthenium 5s and tin 5s are sufficiently large. The ruthenium–tin one-bond coupling constant is determined substantially by the selected transitions from a low-lying occupied molecular orbital, consisting of the ruthenium 5s and the ligand tin 5s orbitals in the bonding phase, e.g., ψ_1 (3), to high-lying unoccupied molecular orbitals, where the ruthenium 5s and the ligand tin 5s orbitals are antibonding, e.g., ψ_8 (9). These transitions account for 108% and 91% of ${}^1\pi(RuSn_{eq})$ of $[Ru(SnCl_3)_6]^{4-}$ and *trans*-$[RuCl_2(SnCl_3)_4]^{4-}$, respectively. Approximately the same orbital energies were obtained for either the unoccupied orbitals ψ_1 (3) (−20.88 eV) and ψ'_1 (**10**) (−19.68 eV) or the unoccupied orbitals ψ_8 (9) (−6.75 eV) and ψ'_9 (**16**) (−6.04 eV), respectively. Moreover, the transitions between these orbitals contributed to ${}^1\pi(RuSn_{eq})$ almost equally.

A remarkable influence of the axial ligands appeared for higher unoccupied orbitals. Let us compare ψ_{11} (**17**) of $[Ru(SnCl_3)_6]^{4-}$ and ψ'_{11} (**18**) of *trans*-$[RuCl_2(SnCl_3)_4]^{4-}$. The energy level of ψ'_{11} (**18**) (25.50 eV) was distinctly lower than that of ψ_{11} (**17**) (30.71 eV). The smaller transition energy of ψ'_1 (**10**) → ψ'_{11} (**18**) than ψ_1 (3) → ψ_{11} (**17**) together with the valence s coefficient products (−0.536 in ψ_{11} (**17**) and −0.564 in ψ'_{11} (**18**), respectively) resulted in a larger contribution for the ψ'_1 (**10**) → ψ'_{11} (**18**) transition (1.80×10^{-3} eV^{-1}) than for ψ_1 (3) → ψ_{11} (**17**) (1.16×10^{-3} eV^{-1}). Since the stabilized MO energy of ψ'_{11} (**18**) is ascribed to the

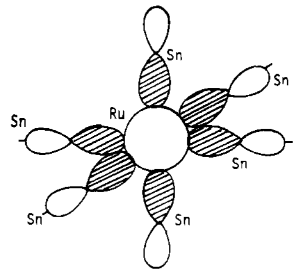

(**17**)

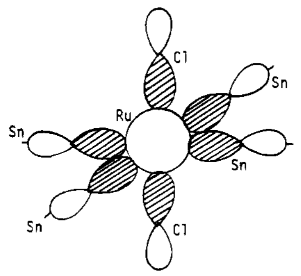

(**18**)

orbital energy levels of chlorine, which are lower than those of the $SnCl_3^-$ ligand, the larger value of $^1\pi(RuSn_{eq})$ in *trans*-$[RuCl_2(SnCl_3)_4]^{4-}$ than in $[Ru(SnCl_3)_6]^{4-}$ again originated from the orbital energy of the axial ligand.

The molecular orbital description on $[RuCl(SnCl_3)_5]^{4-}$ is not as simple as $[Ru(SnCl_3)_6]^{4-}$ or *trans*-$[RuCl_2(SnCl_3)_4]^{4-}$ because of its low symmetry. However, the observed magnitude of its one-bond coupling constant (864 Hz) stands on the position intermediate between that of $[Ru(SnCl_3)_6]^{4-}$ (756 Hz) and *trans*-$[RuCl_2(SnCl_3)_4]^{4-}$ (1123 Hz), reflecting the cis influence of the axial ligand. The observed order in the one-bond coupling constant being larger for $[OsCl(SnCl_3)_5]^{4-}$ (1290 Hz) than for $[Os(SnCl_3)_6]^{4-}$ (1123 Hz) was interpreted similarly in terms of the orbital influence of the axial ligand.

Theoretical interpretation by a perturbation MO method had been given by Shustorovich et al.[18] on the following magnitude order of the one-bond coupling constants in the fluorine-coordinated platinum and tungsten complexes: $[PtF_6]^{2-} > [PtF_5Cl]^{2-} \simeq [PtF_5(OH)]^{2-}$ and $[WF_6] > [WF_5(OMe)] \simeq [WF_5(OPh)]$.[19,20] According to his view, the metal–ligand one-bond coupling constant was determined dominantly by the pair of the occupied and unoccupied orbitals consisting of both the metal s and the ligand s orbitals. A common interpretation is now put for the one-bond coupling constants of the tin(II)-coordinated transition-metal complexes.

(6) Metal–Ligand Coordination Bonding Elucidated from Nuclear Spin Coupling Constants. Less attention has been paid so far to the cis-influence on the metal–ligand coordination bonding in contrast to the trans influence, the extent of which was well described by the EHMO method in terms of the atomic overlap population.[21] Recently, Shustorovich pointed out on the equatorial metal–ligand coordination bonding in d^6 octahedral complexes that the cis influence would be smaller than the trans influence in general owing to the cancellation of contributions between the metal s orbital and d orbital.[22] The occupied molecular orbital, ψ'_1 (**10**), of *trans*-$[RuCl_2(SnCl_3)_4]^{4-}$ well demonstrates this contrasted feature with respect to the metal s and d orbitals, since the equatorial tin ligands and the axial chlorine ligands participate in the same phase with the metal s orbital, whereas the opposite phase is required for the metal d_{z^2} orbital (eq 3).

Table V. Metal–Ligand Overlap Populations in Tin(II)-Coordinated Ruthenium Complexes

	overlap populations			
complex	Ru(s) – Sn(s)	Ru(σ) – Sn(σ)	Ru(π) – Sn(π)	total
$[Ru(SnCl_3)_6]^{4-}$	+0.028	+0.265	+0.053	+0.319
$[RuCl(SnCl_3)_5]^{4-}$	+0.034	+0.288	+0.052	+0.340
trans-$[RuCl_2(SnCl_3)_4]^{4-}$	+0.042	+0.316	+0.050	+0.366

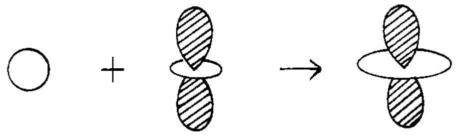

(3)

Both $^1J(MSn_{eq})$ and $^1\pi(MSn_{eq})$ values of tin(II)-coordinated ruthenium and osmium complexes increased by replacing the axial $SnCl_3^-$ ligand with Cl^- (Table IV). In accordance with the monotonous increase in $^1J(MSn_{eq})$, the metal s-ligand s overlap population should become larger by the axial substitution with the other ligand of the lower lying valence orbital.[22] As shown in Table V, an excellent example of this intimate relationship was demonstrated by the tin(II)-coordinated ruthenium complexes. Moreover, the metal–ligand one-bond spin coupling constants were closely related with not only the metal s-ligand s but also the metal σ-ligand σ-overlap populations, as referred to by a lot of coordination compounds.[23] It was also to be noted in Table V that the total overlap populations were dominated by the metal σ–ligand σ components either in magnitude or in trend, while the metal π–ligand π components were nearly constant for these ruthenium complexes. As evident now from the case of the tin(II)-coordinated transition-metal complexes, useful information on the metal–ligand coordination is afforded by the metal–tin one-bond coupling constant and its EHMO elucidation.

From the viewpoint of the valence orbital energy of the axial ligand, its cis influence on the spin coupling constants concerning the equatorial tin ligand atoms were understood satisfactorily. Furthermore, the σ component of the metal–tin coordination was well correlated with the corresponding one-bond spin coupling constant. The present approach, to explore the metal–ligand bonding properties through the nuclear spin coupling constant and its molecular orbital analysis, will be extended to apply to other types of coordination compounds.

Registry No. $[Pt(SnCl_3)_4]^{2-}$, 61421-19-0; $[PtCl(SnCl_3)_3]^{2-}$, 45114-56-5; *cis*-$[PtCl_2(SnCl_3)_2]^{2-}$, 48055-16-9; $[PtCl(PMe_3)_3]^+$, 45114-52-1; $[Ru(SnCl_3)_6]^{4-}$, 82641-14-3; $[RuCl(SnCl_3)_5]^{4-}$, 45264-21-9; *trans*-$[RuCl_2(SnCl_3)_4]^{4-}$, 94293-73-9; $[Os(SnCl_3)_6]^{4-}$, 94241-90-4; $[OsCl(SnCl_3)_5]^{4-}$, 62137-05-7; $[RhH(SnCl_3)_5]^{3-}$, 94987-05-0; $[IrH(SnCl_3)_5]^{3-}$, 96298-29-2; *trans*-$[IrClH(SnCl_3)_4]^{3-}$, 96298-32-7; *trans*-$[IrCl_2(SnCl_3)_4]^{3-}$, 94293-71-7; ^{119}Sn, 15411-62-8; ^{117}Sn, 13981-59-4; ^{99}Ru, 15411-62-8.

---

(18) Shustorovich, E.; Dobosh, P. A. *J. Magn. Reson.* **1980**, *39*, 101.

(19) McFarlane, W.; Noble, A.; Winfield, J. M. *J. Chem. Soc. A* **1971**, 948.

(20) Evans, D. E.; Turner, G. K. *J. Chem. Soc., Dalton Trans.* **1975**, 1238.

(21) Zumdahl, S. Z.; Drago, R. S. *J. Am. Chem. Soc.* **1968**, *90*, 6669.

(22) Shustorovich, E. *Inorg. Chem.* **1979**, *18*, 1030; *J. Am. Chem. Soc.* **1979**, *101*, 792.

(23) Pregosin, P. S.; Kunz, R. W. *^{31}P and ^{13}C NMR of Transition Metal Phosphine Complexes*; Springer-Verlag: New York, 1979.